Hindawi
Geofluids
Volume 2021, Article ID 1250083, 12 pages
https://doi.org/10.1155/2021/1250083

Research Article

Intelligent Prediction Model of the Triaxial Compressive Strength of Rock Subjected to Freeze-Thaw Cycles Based on a Genetic Algorithm and Artificial Neural Network

Xin Xiong,[1,2] **Feng Gao**,[1,2] **Keping Zhou**,[1,2] **Yuxu Gao**,[1] **and Chun Yang**[1,2]

[1]*School of Resources and Safety Engineering, Central South University, Changsha, Hunan 410083, China*
[2]*Research Center for Mining Engineering and Technology in Cold Regions, Central South University, Changsha, Hunan 410083, China*

Correspondence should be addressed to Feng Gao; csugaofeng@csu.edu.cn

Received 11 April 2021; Accepted 3 June 2021; Published 17 June 2021

Academic Editor: Yu Wang

Rock compressive strength is an important mechanical parameter for the design, excavation, and stability analysis of rock mass engineering in cold regions. Accurate and rapid prediction of rock compressive strength has great engineering value in guiding the efficient construction of rock mass engineering in a cold regions. In this study, the prediction of triaxial compressive strength (TCS) for sandstone subjected to freeze-thaw cycles was proposed using a genetic algorithm (GA) and an artificial neural network (ANN). For this purpose, a database including four model inputs, namely, the longitudinal wave velocity, porosity, confining pressure, and number of freeze-thaw cycles, and one output, the TCS of the rock, was established. The structure, initial connection weights, and biases of the ANN were optimized progressively based on GA. After obtaining the optimal GA-ANN model, the performance of the GA-ANN model was compared with that of a simple ANN model. The results revealed that the proposed hybrid GA-ANN model had a higher accuracy in predicting the testing datasets than the simple ANN model: the root mean square error (RMSE), mean absolute error (MAE), and R squared (R^2) were equal to 1.083, 0.893, and 0.993, respectively, for the hybrid GA-ANN model, while the corresponding values were 2.676, 2.153, and 0.952 for the simple ANN model.

1. Introduction

The distribution of permafrost and seasonal permafrost in China, mainly in the west and north, accounts for more than 70% of the total land area [1]. With Western development and the in-depth implementation of the "belt and road" national strategy, mineral resource development and engineering construction in cold regions are steadily increasing [2]. The rock masses addressed in geotechnical engineering in cold regions are subject to freeze-thaw cycling caused by day-night and seasonal temperature changes [3, 4]. Because of the unique stress field and environment, microdefects inside the rock will continue to form and expand. The macroscopic effect of the damage accumulation is represented by the deformation and destruction of the rock, which causes potential damage to rock mass engineering. Therefore, the study of the mechanical properties of rocks in cold regions has important engineering value for the stability of rock mass engineering.

The triaxial compressive strength (TCS) of rock is a key rock mechanics parameter to be considered in rock mass engineering. It is considered in the design, excavation, and support of rock mass engineering. Many researchers have conducted a considerable amount of research on the mechanical properties of rocks subjected to freeze-thaw cycles based on laboratory tests. Tan et al. [5] and Hosseini and Khodayari [6] performed triaxial compression tests of granite and sandstone, respectively, subjected to different numbers of freeze-thaw cycles. It was found that with the increase in the number of freeze-thaw cycles, the TCS of the rock decreases, and with the increase in the confining pressure, the TCS of the rock increases. Shen and Wang [7]

analyzed the freeze-thaw damage mechanism of rocks in cold regions, expounded the freeze-thaw damage process of the rock, and analyzed the influence of external influencing factors such as the freeze-thaw temperature, number of freeze-thaw cycles, and stress state on rock freeze-thaw damage in detail. Bai et al. [8] carried out uniaxial and triaxial compression tests of saturated sandstone at different frozen temperatures. The effects of frozen temperature on peak strength, elastic modulus, cohesion, and internal friction angle were analyzed, and the relationships between the confining pressure and the peak strength and elastic modulus were obtained. These work has important guiding significance for the study of the factors influencing the compressive strength of rock in freeze-thaw environments.

Although many of these influencing factors have been investigated in freeze-thaw experiments, it is difficult to obtain the TCS of rocks subjected to any number of freeze-thaw cycles because of the lack of a precise prediction model. This has driven scholars to search for easy and reliable methods to predict the mechanical properties of rocks subjected to freeze-thaw cycles. Bayram [9] developed a statistical model to estimate the reduction in the uniaxial compressive strength of limestone after freeze-thaw cycle treatment. İnce and Fener [10] investigated various rock index properties after freeze-thaw cycle treatment, including the dry density, ultrasonic velocity, point load strength, and slake-durability test indices, and proposed a statistical model to predict the uniaxial compressive strength of deteriorated pyroclastic rocks. Liu et al. [11] improved an empirical equation to determine the uniaxial compressive strength of rocks subjected to freeze-thaw cycles based on a fatigue damage model. Fu et al. [12] and Seyed Mousavi et al. [13] proposed a TCS prediction model for transversely isotropic rocks subjected to freeze-thaw cycles based on the single discontinuity theory. However, the unknown parameters in those models should be determined by experimental tests. Because the experiment is expensive, time-consuming, and laborious, it is difficult to provide rapid guidance for engineering design and construction. In addition, the prediction models are based on specific hypothetical function forms, the prediction results show good consistency under specific conditions, but the prediction results are poor when these models are applied to other rock types.

It was highlighted that artificial intelligence (AI) techniques have an impressive potential for use in geotechnical engineering [14–16], especially in solving rock mechanics problems [17, 18]. To the best of the authors' knowledge, no study has developed a hybrid GA-ANN model for TCS prediction of rocks subjected to freeze-thaw cycles. Therefore, in this paper, to solve this problem, a hybrid GA-ANN prediction model is constructed and proposed. First, a database of 60 datasets is prepared and used in the modeling. From this database, the longitudinal wave velocity, porosity, confining pressure, and number of freeze-thaw cycles are utilized as model inputs. Furthermore, the developed models, including a simple ANN model and hybrid GA-ANN model, are compared to select the best model for estimating TCS of rocks subjected to freeze-thaw cycles.

2. Laboratory Tests and Collect Datasets

The rock specimens used in this test were sandstone taken from the Jiama open-pit copper mine located in the Tibet Autonomous Region of China. According to the Commission on Testing Methods of the International Society for Rock Mechanics, all the sandstone specimens were cylindrical samples with diameters of 50 mm and the end surfaces were polished to ensure that the flatness was less than 0.05 mm. Careful preparations ensured that the maximum deviations of the specimen diameters and heights were less than 0.3 mm and that the vertical deviation was less than 0.25°. Sixty sandstone specimens with a length/diameter ratio of 2.0 were used in the freeze-thaw cycle tests and conventional triaxial compression tests.

2.1. Determination of Input and Output Variables. When using machine learning to predict rock mechanical properties, the choice of input variables (influencing factors) is very important. The selection of general input variables needs to follow the following rules: (1) the physical meaning of the parameters is clear, (2) the parameter values are easy to obtain, and (3) the characteristics of the output variables can be comprehensively reflected. The TCS of the rock is combined with other factors, such as the pore structure, deposition environment, and ground stress. In this paper, we establish a lossless intensity prediction model and then select variables that are easy to measure and control, such as the confining pressure, porosity, longitudinal wave velocity, and number of freeze-thaw cycles, as input variables to predict the TCS of the sandstone. Among them, the confining pressure reflects the magnitude of rock mass stress, the porosity and longitudinal wave velocity reflect the rock integrity, and the number of freeze-thaw cycles reflects the natural environmental factors in alpine regions.

2.1.1. Determination of Freeze-Thaw Cycles. Because of the day-night and seasonal temperature changes, rocks in cold regions undergo repeated freeze-thaw cycling. The 60 sandstone specimens were divided into 5 groups (labeled A through E), and each group comprised 12 rock specimens (labeled 1 through 12). The sandstone specimens from groups A, B, C, D, and E were treated for 0 cycles, 10 cycles, 20 cycles, 30 cycles, and 40 cycles, respectively. The freeze-thaw weathering process was simulated with a TDS-300 automatic freeze-thaw test machine (Figure 1(a)). Based on the local climate of the mine site, one freeze-thaw weathering cycle in our tests included freezing the saturated rock specimens at −20°C for four hours and then thawing them in water at +20°C for four hours. Therefore, one freeze-thaw weathering cycle lasted for 10 hours, including the cooling time and warming time.

2.1.2. Determination of Porosity. Porosity is an important quantitative criterion for rock cracks and voids. There are many microcracks and microvoids inside rocks. When the temperature drops below 0°C, the water in these microdefects freezes into ice and its volume expands by approximately 9%, which produces pressure on the pore walls. When the pressure on the walls exceeds the tensile strength of the rock

(1) Control panel
(2) Water tank
(3) Freeze-thaw cavity

(a)

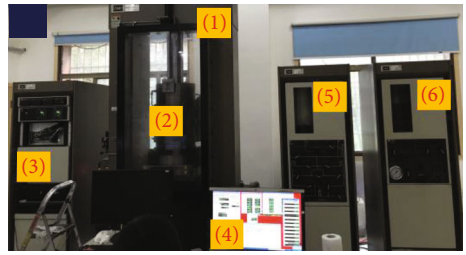

(1) Counterforce frame
(2) Confining cylinder
(3) Power source
(4) Control interface
(5) Water pressure system
(6) Oil pressure system

(b)

Figure 1: Experimental apparatus. (a) TDS-300 automatic freeze-thaw test machine. (b) MTS815 electrohydraulic servocontrolled rock testing machine.

[19], it causes defect development and the porosity increases. When the frozen water melts, water will be absorbed into the defect spaces before the next freezing step [20]. Repeated freeze-thaw cycles can cause rapid deterioration of the physical and mechanical properties of rocks. Therefore, porosity has a great influence on rock strength after freeze-thaw cycle treatment. According to the literature [21, 22], porosity can be measured by nuclear magnetic resonance (NMR). Hence, in this study, after the corresponding freeze-thaw cycles of the specimens were completed, the AniMR-150 NMR imaging system was used to perform measurements.

2.1.3. Determination of Longitudinal Wave Velocity. Stress influences the distribution and orientation of microcracks inside rocks, which leads to a change in the macroscopic physical properties and the longitudinal wave velocity of the rock. Therefore, longitudinal wave velocity is a powerful indicator of the distribution of cracks inside rocks. After the corresponding freeze-thaw cycles of the specimens were completed and dried, the longitudinal wave velocity of the sandstone specimens was determined using an HS-YS4A rock acoustic wave parameter test system.

2.1.4. Determination of Confining Pressure. Confining pressure is an important factor affecting the TCS of rock. Therefore, in this study, based on the in situ geological data and laboratory conditions, the tested confining pressures were 3 MPa, 6 MPa, 9 MPa, and 12 MPa, corresponding to specimens 1–3, 4–6, 7–9, and 10–12 in each group.

2.1.5. Determination of Triaxial Compressive Strength. The TCS of the rock specimens was determined by performing conventional triaxial compression tests. Each sandstone specimen was compressed at a constant confining pressure, and then, the axial load was increased until the specimen failed. The conventional triaxial compression tests were conducted on an MTS815 electrohydraulic servocontrolled rock testing machine (as shown in Figure 1(b)) with a maximum loading capability of 2600 kN. The displacement-control loading mode was used in the experiment, and the loading rate was 0.1 mm/min.

Figure 2 shows the TCS results of the sandstone specimens under different combinations of influencing variables (number of freeze-thaw cycles and confining pressure) with a detailed illustration of the specimens in group E (40 cycles). As expected, the TCS of the sandstone decreased with increasing number of freeze-thaw cycles; the TCS of the sandstone increased with increasing confining pressure. The strength characteristics of the sandstone under different influencing variables found in this paper agree with findings presented in the literature [5, 6].

2.2. Database. As mentioned above, to achieve the goal of this study, a series of rock tests, including tests of the porosity, longitudinal wave velocity, and TCS, were carried out on sandstone specimens. In total, a database of 60 datasets was prepared for further analyses. More statistical information regarding the established database, i.e., the maximum, minimum, and mean results, is presented in Table 1.

3. Methods

3.1. Artificial Neural Network. ANNs are one of the most important methods in artificial intelligence. ANN is a multilayer perceptron model composed of directional interconnected neurons and is used to determine the nonlinear relationship between input variables and output variables. Each neuron is a basic computing unit such as $y = \max(0, \sum_i w_i x_i + b)$, in which $\{x_i\}$ is the input value of the neuron, $\{w_i\}$ is the corresponding weight value of each input variable, b is the bias, and y is the output of the neuron. For each neuron, a summation operation is first performed for the inputs that are multiplied by the appropriate weights, and then, the output is produced with the use of an "activation function." The output should be in the range [0, 1] and exhibit a behavior comparable to that of the activation of a biological neuron [23]. Therefore, a function with a sigmoid curve shape, such as a hyperbolic tangent function, is selected. The basic element of an ANN is the determination

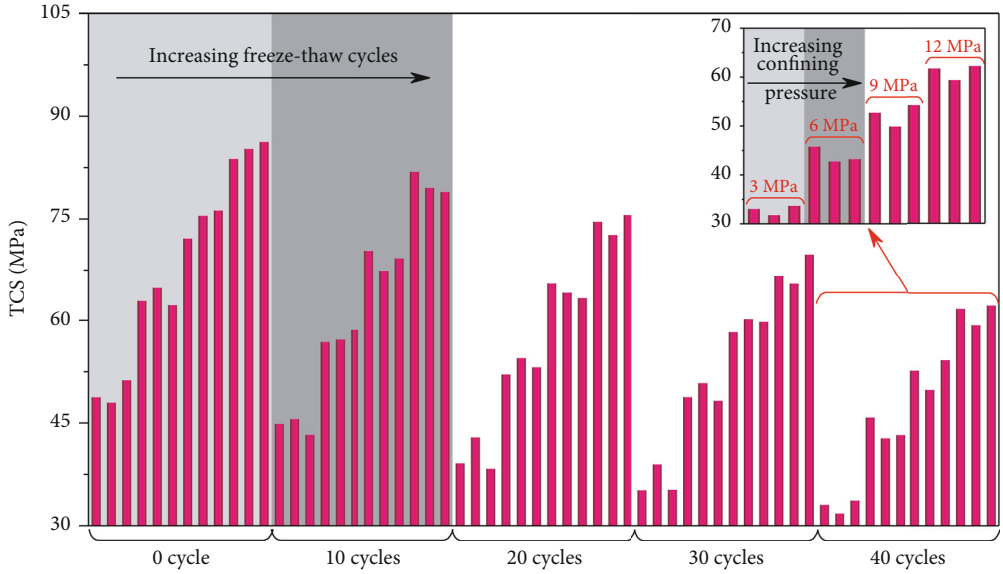

Figure 2: TCS test results with enlarged figures for sandstone specimens in group E (40 cycles).

Table 1: Statistical information regarding the established database.

Parameter	Unit	Category	Min	Max	Mean
Number of freeze-thaw cycles	Times	Input	0	40	20
Porosity	%	Input	7.49	10.23	8.67
Longitudinal wave velocity	m/s	Input	1961.53	2604.19	2327.91
Confining pressure	MPa	Input	3.0	12.0	7.5
TCS	MPa	Output	31.78	86.83	58.11

of weights, which are related to the connection mode between neurons of different layers, that is, the ANN structure [24]. At present, there are many methods available to determine the ANN structure such as the empirical formula method [25] and coupling optimization algorithm [26].

The ANN training process can be divided into three steps. Datasets are usually divided into three sets: a training set, validation set, and test set. First, the weights and biases are determined based on the training set; then, the weights and biases are adjusted by feedback based on the validation set until the error stops falling; finally, the generalization ability of the model, that is, the ability to predict unknown inputs, is tested by the test set. The RMSE is usually used to reflect the prediction error of an ANN, as shown in equation (2).

3.2. Genetic Algorithm. The genetic algorithm is a computational model that simulates the natural selection and genetic mechanism of Darwin's biological evolution theory. It solves for an optimal solution by simulating the natural evolution process. It was first proposed by Holland [27] in 1973 and was further developed by researchers such as Goldberg [28]. Since its inception, GA has been successfully applied in various fields and has been used to solve different optimization problems, whether the objective (fitness) function is static or dynamic, linear or nonlinear, continuous or discontinuous. However, the rational mathematical expression of the fitness function and gene selection method are the key points in the application of genetic algorithms. In addition, the improper selection of population size and genetic operator rate will also affect the convergence of the algorithm. Therefore, a reasonable fitness function and appropriate parameter settings should be selected for different optimization objectives. The implementation process of GA is shown in Figure 3(a).

Generally, the process of the standard genetic algorithm can be described by the following steps:

(1) In the initial population, n chromosomes are randomly generated, i.e., n solutions of the objective function

(2) Evaluate all chromosomes in the initial population, and rank them according to the objective function

(3) Selection operator: according to the specific selection method, chromosomes with high adaptability are selected to enter the next generation population and some chromosomes are eliminated

(4) Crossover operator: random selection of parent chromosomes and exchange of gene fragments to generate new chromosomes (children) in the next generation to supplement the individuals eliminated in the selection, as shown in Figure 3(b)

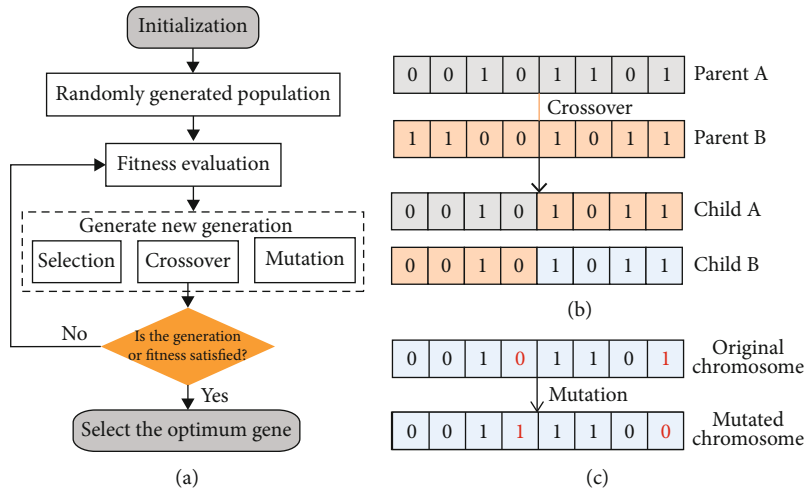

Figure 3: GA process and interpretation.

(5) Mutation operator: to simulate the gene mutation behavior in population reproduction, some genes of the chromosomes (in a certain proportion) of each generation are mutated, as shown in Figure 3(c). Increasing the diversity of chromosomes with population iteration can effectively avoid falling into the dilemma of local optimal solutions

(6) Repeat steps 2 to 5 until a predetermined stopping condition is satisfied, usually to the maximum multiplication algebra set in advance. Finally, the chromosome with the highest fitness is selected as the optimal solution of the objective function and the chromosome is transformed into the actual solution by coding language

There are many choice operators in GA, and the mechanisms are different. Among them, roulette selection, elite selection, and tournament selection are the most popular. The roulette selection method is a replay-type random sampling method. The probability that a chromosome in a population is selected is proportional to its corresponding fitness (adaptive function value). By accumulating and then normalizing the fitness values of all the individuals in the population and generating random numbers, according to the area where the random numbers fall, select the corresponding individuals as parents. The elite selection method, also known as the best retention method, completely copies the most adaptive chromosomes in the current population to the next-generation group. The tournament selection method is also called the random competition selection method. Each time, a pair of chromosomes is selected by roulette, competition occurs, and the chromosome with the highest fitness is selected to enter the next generation until all the chromosomes in the tournament have participated and the preset threshold is reached. The elite selection method and the tournament selection method are improved versions of the roulette selection method, and their selection error is better than that of the roulette selection method. The retention mechanism of the elite selection method makes it difficult to guarantee chromosome diversity in reproduction, so a certain probability will lead to a local optimal solution. The literature [29] compares these three selection operators to prove that the tournament selection method performs better than the other two methods. Therefore, the tournament method is used here as the embedded algorithm of the selection operator.

3.3. GA-ANN Combination. As mentioned above, the main problems that ANN needs to solve in the application include the following: (1) determining the optimal parameters in a machine learning algorithm. Most studies use the grid search method [30] or empirical formula method [24], but both of these methods have serious defects that are difficult to overcome: the grid search method is an exhaustive search method. The possible values of each parameter are arranged and combined, and all the combinations are used as input parameters for the modeling, which is time-consuming and inefficient. The neural network structure based on the empirical formula method has a good generalization ability, but the application items and data distribution of the neural network often have great differences because the accuracy of the model constructed by this method is often poor. (2) Determine the optimal initial weights and biases. The default initial weights and biases are random numbers between $[-1, 1]$. The blindness of their setting will increase the number of iterations in model training, which will slow the convergence speed of the model and seriously affect the accuracy and application effect of the model. Therefore, it is necessary to solve such problems with an optimization algorithm.

Regarding the optimization study of ANNs, researchers have adopted a method of coupling GA and ANN in various scientific studies, namely, the GA-ANN method. Arifovic and Gencay [29] used GA to optimize the neural network structure and verified that this method is superior to Schwarz and Akaike's empirical criteria. Bahnsen and Gonzalez [31] used not only GA to tune the number of hidden layers and neurons but also the type of activation function for hidden and output layers and the bias terms, and compared with

the optimization performance of binary particle swarm optimization algorithm (BPSO), the research proved that the GA optimization approach was superior to that of the default process of network structure determination and that this approach led to a solution that is very close to the global optimum based on GA-MLP. Boithias et al. [32] used GA-ANN to predict indoor discomfort and energy consumption. They used GA to optimize the parameters of the ANN structure and training process. First, the GA was used to realize variable selection and the variables that have a small influence on ANN training was eliminated. Finally, a model with considerable accuracy was obtained. Idrissi et al. [33] used GA to optimize the ANN, with a view to minimize the number of hidden layers and neurons while having the lowest MSE. Jeong et al. [34] employed a generalized additive model (GAM) and GA to tune the structure and decay coefficient of the ANN model. Based on the optimal structure and decay coefficient value, the proposed approach was compared to other classification methods, as well as to a nontuned ANN, and it was found that the GA-ANN performed better than other approaches. Efkolidis et al. [23] used GA-ANN to predict the thrust (Fz) and torque (Mz) during the drilling of St60 work pieces. The structure, connection weights, and training algorithms of an ANN were optimized in turn based on GA. The superiority of ANN progressive optimization is verified. However, in this paper, when considering only the prediction accuracy, the double-hidden-layer structure is the optimal model but the authors have not further optimized the multiple-hidden-layer ANN model.

Of the many researchers of GA-ANN, few scholars have considered progressive optimization from the aspects of the ANN structure and connection weight, especially after determining the optimal structure of a multiple-hidden-layer ANN. Few studies have further optimized the initial connection weights and biases. In view of this, a new GA-ANN method is proposed in this paper to accurately predict the TCS of sandstone subjected to freeze-thaw cycles. The model explores the nonlinear relationship between TCS (output) and confining pressure, number of freeze-thaw cycles, porosity, and longitudinal wave velocity (four inputs). The research includes two-step optimization of the structure, weights and biases of an ANN by GA, and the prediction performance is compared with the ANN model created in a simpler way. Therefore, this paper studies the optimal structure of an ANN for predicting the TCS of sandstone and compares it with the empirical formula method. Then, on the basis of the ANN optimal structure, the initial connection weights and biases are further optimized and a final GA-ANN model is obtained.

4. Details of the Development of ANN Models

4.1. Data Preprocessing. It can be seen from the data statistics in Table 1 that there are large differences between the dimensions and magnitudes of the five variables. To speed up the learning of neural networks and avoid singular samples, before the ANN modeling, the dataset should be normalized by equation (1) [35] and the output of the prediction result should be inversely normalized for comparison with the experimental values.

$$X_{\text{norm}} = \frac{(X - X_{\min})}{(X_{\max} - X_{\min})}, \tag{1}$$

where X and X_{norm} are the experimental value and the normalized value, respectively, and $X_{\max}$ and $X_{\min}$ are the maximum value and the minimum value, respectively.

In addition, in supervised learning, the dataset needs to be divided into training samples (i.e., training set and validation set) and test samples, wherein the training samples are used to optimize the model learning and model parameter tuning; the test samples are used to test the generalization ability and reflect the prediction performance of the model. Based on the analysis results from the literature [36], the dataset is divided into a training sample set and a test sample set according to a ratio of 7 : 3.

4.2. Verification Method. The k-fold crossvalidation method is applied as a verification method for model training. In k-fold crossvalidation, the training dataset D is divided into k mutually exclusive subsets of similar size: $D = D_1 \cup D_2 \cup \cdots \cup D_k$, and $D_i \cap D_j = \varphi(i \neq j)$. To reduce the impact of sample randomness on the prediction model, each subset maintains the consistency of the data distribution as much as possible, i.e., by stratified sampling. This subset is selected as the verification sample, the remaining $k - 1$ sets are used as the training set, and finally, the mean value of the k verification results is returned. The amount of data in this paper is small, and a 5-fold crossvalidation method is selected.

4.3. Simple ANN Model. The ANN capabilities are dependent directly on the ANN structure [16]. Therefore, to establish an ideal neural network model, a structural optimization design must be carried out. As mentioned above, there are many studies on empirical formulas of the ANN model structure. The empirical formula method suggests that for small- and medium-sized datasets, an ANN model with a single hidden layer can evaluate any nonlinear relationship [37, 38]. Table 2 lists several ANN structure empirical formulas for calculating the number of neurons in a single hidden layer. In this study, four input variables and one output variable were used in the prediction model; hence, $N_i = 4$ and $N_0 = 1$. It can be seen from the calculation that the ANN structure constructed by several different formulas is very different.

The most well-recognized formula is from Zhang et al. [39]. Therefore, based on the trial-and-error method, 11 single-hidden-layer ANN models for predicting TCS were constructed and the number of neurons in the hidden layer ranged from 3 to 13. According to the study results from the literature [23], the Levenberg-Marquardt (LM) algorithm was selected as the training algorithm. Taking RMSE as the ANN model performance measurement standard, the lower the RMSE is, the better the model performance. To reduce the error, all the ANN models were trained five times and the average RMSE values were considered in the following analysis. Table 3 shows that model 10 has the best prediction performance for the TCS of sandstone subjected to freeze-thaw cycles, and the corresponding RMSE (3.52) is the

Table 2: Empirical formulas of the ANN structure.

Reference	Equations	Computational results	Parameter
Zhang [39]	$\sqrt{N_i + N_0} + a, a \in [0, 10]$	$3 \le n \le 13$	N_i and N_0 are the numbers of neurons in the input layer and output layer, respectively, which are both 3 in these paper.
Hecht-Nielsen [37]	$\le 2 \times N_i + 1$	$n \le 9$	
Ripley [40]	$(N_i + N_0)/2$	$n = 3$	
Paola [41]	$\left(2 + N_0 \times N_i + 0.5N_0 \times \left(N_0^2 + N_i\right) - 3\right)/N_i + N_0$	$n = 8$	
Wang [42]	$2N_i/3$	$n = 3$	
Masters [43]	$\sqrt{N_i \times N_0}$	$n = 3$	
Kaastra and Boyd [44], Kanellopoulos and Wilkinson [45]	$2N_i$	$n = 8$	

lowest. The structure of the model is (4-12-1). Later, we use (4-12-1) as the optimal model for TCS prediction with a simple ANN model and compare its performance with that of the ANN model based on GA structure optimization.

4.4. GA-ANN Model. The GA-ANN presented in this paper summarizes the process of determining the optimum network structure and the optimum initial weights and biases for predicting the TCS of sandstone subjected to freeze-thaw cycles. The prediction errors are minimized by changing the network structure and other parameters. This process will be implemented in two steps in this section. The GA parameter settings in the two-step optimization process are shown in Table 4.

4.4.1. ANN Structure Tuning Based on GA. GA is a powerful optimization technique for finding a global optimum in a multidimensional searching space. The global optimization ability of the GA algorithm was used to perform ANN structural tuning. The global search scope of the ANN structure should be determined first. If the search range is set too large, the number of calculations will be too large and the convergence speed will be slow. When the search range is set too small, the optimal ANN structure may be missed. Therefore, setting reasonable search boundaries is important for the performance of the model. The expert-level model can be obtained by setting appropriate parameters. Therefore, according to the relevant reference [26], the learning rate and structural boundary settings of the ANN are as follows (see Table 5). In this process, because the performance of the model is inversely related to the RMSE, the fitness function is set to the reciprocal form of the RMSE, i.e., 1/RMSE. According to the literature [46], the number of maximum generations is set to 20, the selection operator is the tournament selection method, the crossover rate and the mutation rate are 0.8 and 0.1, respectively, and the population number is 200. The process stops when it iterates to the maximum reproductive value (20). See Table 4 for the details of the GA.

Figure 4 shows the changing process of the minimum RMSE (corresponding to the optimal chromosome) in each generation of populations when using different numbers of hidden layers. It can be seen from the four curves that the minimum RMSE value of each generation shows a significant downward trend with population reproduction, which proves the effectiveness of the GA for the structural optimization of ANN. Figure 4(a) is the optimization process of the ANN model structure for predicting TCS of sandstone subjected to freeze-thaw cycles. After one iteration, the minimum RMSE of the population is greatly reduced; after that, the minimum RMSE in every generation progressively reduces in the first 15 iterations and the lowest RMSE was achieved by the ANN model with two hidden layers (14 neurons in the first layer and 11 neurons in the second). The RMSE value (1.562) is much lower than the minimum RMSE (3.52) corresponding to the simple ANN based on the empirical formula method. Although the simple ANN can map any nonlinear relationship, it is not the optimal choice. Figure 4(b) shows the ANN structure after the optimization of the GA, which is used for further optimization, as described below. Therefore, the optimal structure of the ANN is determined to be (4-14-11-1).

4.4.2. ANN Initial Connection Weight and Bias Tuning Based on GA. After determining the ANN structure, the initial connection weights and biases of the ANN are optimized. The initial connection weights and biases are generally chosen as random numbers between (−1, 1). Because of the randomness of the initial weight and bias setting process, the learning time and final connection weights of the model keep changing due to the number of training iterations. Therefore, even if specific ANN structural parameters are determined, the trained final ANN model is not unique, which often leads to the ANN model falling into a local optimal deadlock, thus affecting the accuracy of the model. In addition, the blindness of the initial weight and bias setting will increase the number of iterations of the model training, resulting in slower convergence of the model. This process seriously affects the accuracy and application effect of the model. Therefore, it is necessary to further apply GA to tune the initial weights and biases of the ANN model, which possesses the optimal structure.

The number of optimization objects (connection weights and biases) is consistent with the length of the chromosomes in the GA. For the ANN structure (4-14-11-1) identified above, the connection weights and biases of the model are calculated by stratification and the total number is $(4 \times 14) + (14 \times 11) + (11 \times 1) + (14 + 11 + 1) = 247$, where (4×14) is the connection weights between the 4 input neurons and

Table 3: Simple ANN optimal network structure and prediction results.

Model no.	TCS Nodes in hidden layer	Average RMSE
1	3	9.266
2	4	6.165
3	5	7.381
4	6	5.244
5	7	5.038
6	8	4.157
7	9	5.284
8	10	4.753
9	11	5.021
10	12	3.522
11	13	4.320

the 14 hidden neurons in the first hidden layer, (14×11) is the connection weights between the 14 neurons in the first hidden layer and the 11 neurons in the second hidden layer, and (11×1) is the connection weights between the 11 neurons in the second hidden layer and the output neuron; 14, 11, and 1 are the total number of biases on the first hidden layer, the second hidden layer, and output layer, respectively. Considering that the chromosomes are a floating point type and that the number of chromosomes is large, to determine the optimal population number, the population size should be 50, 100, 150, and 200 in turn and the maximum iteration should be set to 500 to ensure the realization of the global optimal solution. The parameters of GA are specified in Table 4.

Figure 5 shows the iterative process of the initial weight and bias tuning of the ANN model with the optimal structure. Although there are great differences among the four iteration curves (dashed lines) corresponding to different population sizes, the maximum RMSE is less than the RMSE (1.562). The RMSE corresponding to population chromosome number 150 is the lowest. Therefore, the population size of the GA-ANN model selected in the following training is 150. Compared with the optimization results in the previous section, the prediction error of the ANN is greatly reduced and the model performance is improved.

5. Evaluation of the Performance of the Model

In the process of GA-ANN model training, the inclusion of the GA can significantly improve the prediction performance of ANN. The database is randomly divided into a training set and testing set at a ratio of 7 : 3 and repeated five times. Based on the five datasets, five ANN models and five GA-ANN models are established with the optimal parameters determined above. To further verify the superiority of GA-ANN, RMSE, MAE, and R^2 are used to test the performance of the model. The calculation methods are as follows:

$$\mathrm{RMSE} = \sqrt{\frac{1}{n}\sum_{i=1}^{n}\left(y_{\mathrm{exp},i} - y_{\mathrm{pred},i}\right)^2}, \tag{2}$$

$$\mathrm{MAE} = \frac{1}{n}\sum_{i=1}^{n}\left|y_{\mathrm{exp},i} - y_{\mathrm{pred},i}\right|, \tag{3}$$

$$R^2 = 1 - \frac{\sum_{i=1}^{n}\left(y_{\mathrm{pred},i} - y_{\mathrm{exp},i}\right)^2}{\sum_{i=1}^{n}\left(y_{\mathrm{exp},i} - \overline{y_{\mathrm{exp},i}}\right)^2}, \tag{4}$$

where n is the number of test samples, $y_{\mathrm{exp},i}$ is the experimental value, $y_{\mathrm{pred},i}$ is the predicted value of the test samples, and $\overline{y_{\mathrm{exp},i}}$ is the average value of the test samples. The RMSE and MAE are used to measure the degree of deviation between the predicted value and the true value. The smaller the RMSE or MAE is, the smaller the prediction error of the model. R^2 is between [0, 1], and the larger R^2 is, the better the prediction ability of the model.

Table 6 lists the obtained values of the performance indices for the proposed simple ANN and hybrid GA-ANN models. The prediction of testing data can reflect the application performance and generalization ability of the model; hence, these results are presented based on the test set. To select the best datasets of ANN and GA-ANN, a ranking technique proposed by Zorlu et al. [47] was used. As shown in Table 6, when a GA is incorporated into the ANN, the prediction performance of the model is significantly improved. According to the total score, the ANN based on the empirical formula has the best prediction performance for dataset 2, for which the RMSE, MAE, and R^2 are 2.676, 2.153, and 0.952, respectively. The GA-ANN based on dataset 5 has the best performance, with RMSE, MAE, and R^2 scores of 1.083, 0.893, and 0.993, respectively. The performance of the GA-ANN model is better than that of the simple ANN model based on any evaluation criterion.

Based on datasets 2 and 5, with the true value (experimental value) as the abscissa and the predicted value as the ordinate, a scatter point figure is made (Figure 6). Figures 6(a) and 6(b) show the relationship between the predicted and measured values of the simple ANN model and GA-ANN model, respectively. Line $y = x$ is the ideal prediction model. The closer the scatter points are to the straight line, the more accurate the prediction results are. Comparisons show that the fitness between the scatter points and ideal straight lines in Figure 6(b) is much greater than that in Figure 6(a).

6. Superiority and Limitations

The primary strength of this study is the verification of the GA-ANN method for the prediction of TCS of sandstone subjected to freeze-thaw cycles. Advantages of the GA-ANN method over conventional experimental tests include its low cost, low time consumption, and nondestructive process, which will become more evident when a larger rock dataset is available. Even compared with existing models, the GA-ANN still has the following advantages: (1) the

Table 4: GA parameter settings.

GA parameter	Values	
Scenarios	Optimization of ANN structure	Optimization of initial weights and biases
Fitness function	1/RMSE	1/RMSE
Selection method	Tour	Tour
Genetic possibility	Crossover (0.8), mutation (0.1)	Crossover (0.8), mutation (0.1)
Stop criteria	Maximum generation	Maximum generation
Number of chromosomes	200	50/100/150/200
Type of chromosomes	Integer	Float
Number of generation	20	500

Table 5: ANN parameters and tuning range.

Hyper parameters	Explanation	Type	Tuning range
Max_neuron	Maximum number of neurons in every hidden layer	Integer	1–40
Number_hidden_layers	Maximum number of hidden layers	Integer	1–4
Input_layer_neuron	Number of neurons in the input layer	Integer	3
Output_layer_neuron	Number of neurons in the output layer	Integer	3
Learning rate	Weight reduction due to updating in feedback training	Float	0.01

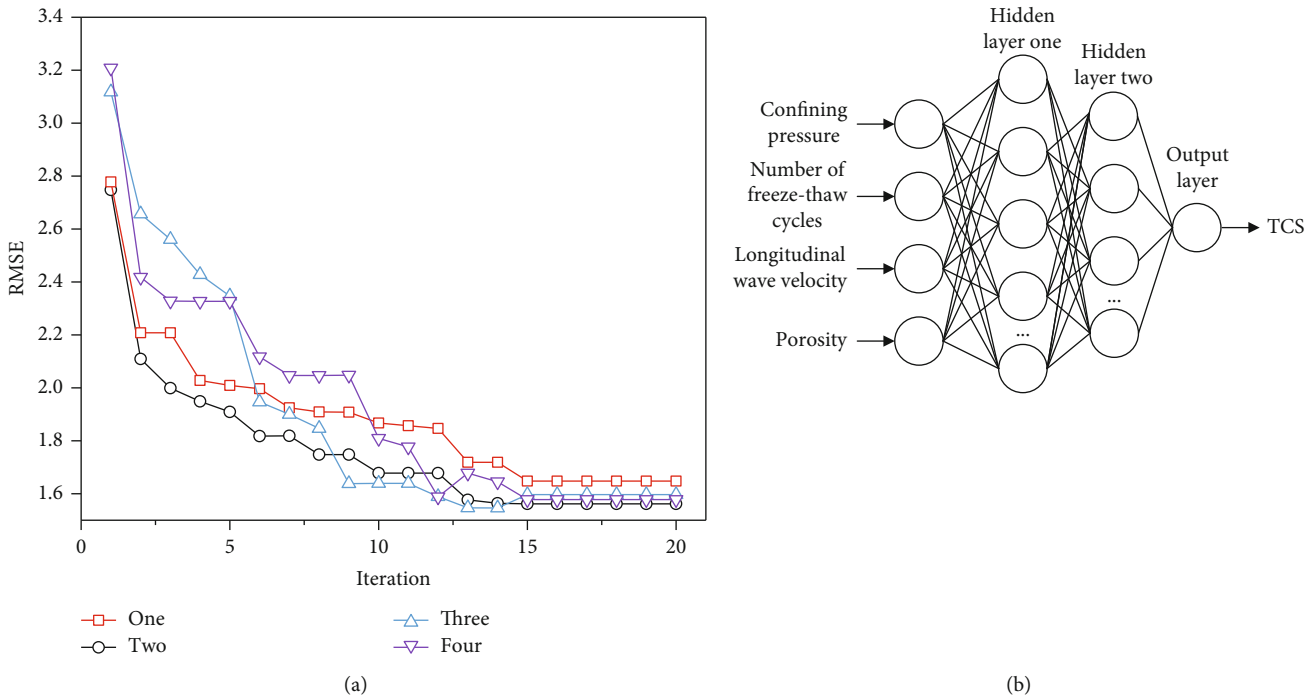

Figure 4: Structure parameter tuning: (a) minimum RMSE versus iteration with 1–4 hidden layers; (b) optimal ANN structure.

GA-ANN method requires no mechanical tests, as the prediction is made directly from the influencing variables of the TCS, (2) the generalization capability of the GA-ANN method might be better than existing models, which need to be fit based on a specific dataset, and a general model can be easily built and updated using a more comprehensive dataset, and (3) most importantly, such predictions can promote the establishment of "intelligent management for engineering" in the future.

The omission of other influencing variables of the TCS of sandstone, such as the addition of freeze-thaw temperature, rock mineralogical composition, and water saturation degree, is a clear limitation of the current study. A larger dataset containing more types and mineralogical composition variables

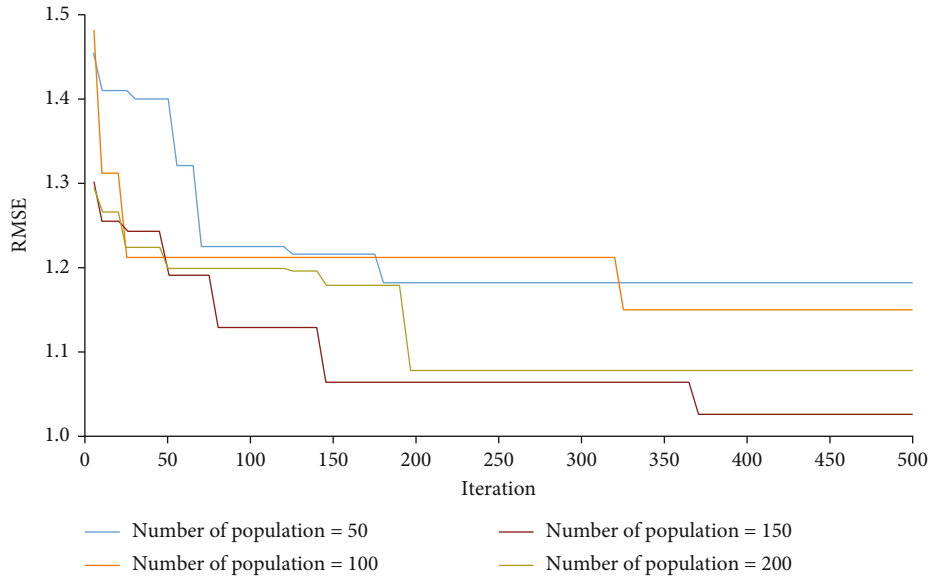

Figure 5: Initial connection weight and bias parameter tuning.

Table 6: Results of the performance indices of the ANN and GA-ANN models.

Method	Model	RMSE	MAE	R^2	Rating for RMSE	Rating for MAE	Rating for R^2	Rank value
ANN	1	3.408	2.395	0.925	1	4	1	6
	2	2.676	2.153	0.952	5	5	3	13*
	3	3.123	2.426	0.937	4	3	2	9
	4	3.301	2.524	0.953	2	2	4	8
	5	3.186	2.626	0.958	3	1	5	9
GA-ANN	1	1.139	0.866	0.992	4	5	4	13
	2	1.165	0.899	0.991	3	3	3	9
	3	1.302	1.004	0.989	1	1	1	3
	4	1.206	0.949	0.990	2	2	2	6
	5	1.083	0.893	0.993	5	4	5	14*

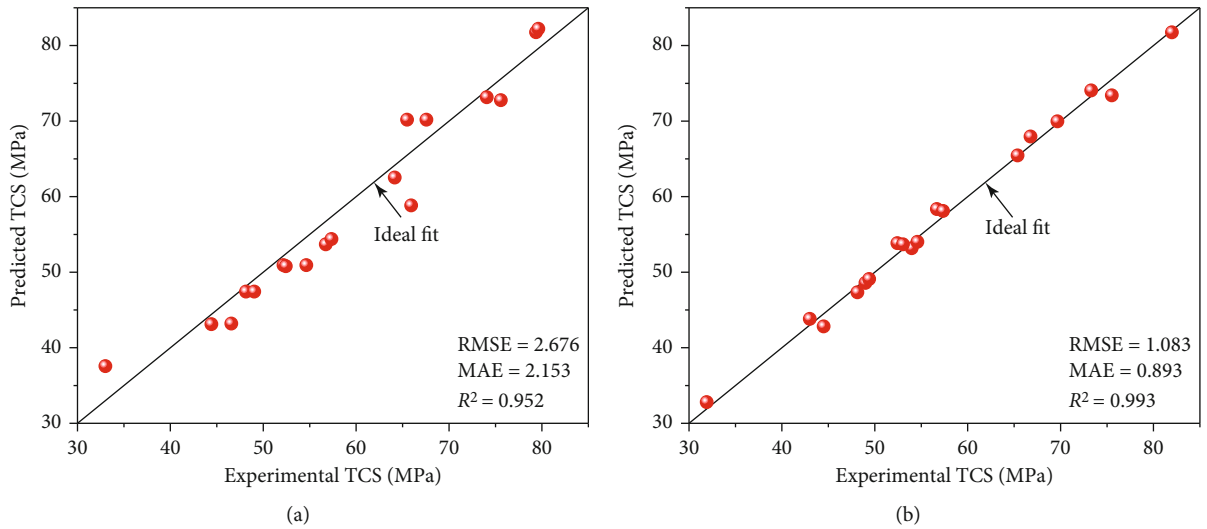

Figure 6: Comparison of the predicted and experimental TCS values: (a) simple ANN model; (b) GA-ANN model.

of rocks is being collected in the hope that the generalization capability of the trained ANN model can be improved once physical-mechanical characteristics are used as inputs.

7. Conclusions

This paper established a new AI model (GA-ANN) for estimating the TCS of sandstone subjected to freeze-thaw cycles. A database consisting of 60 datasets was prepared, and in each dataset, the longitudinal wave velocity, porosity, confining pressure, and number of freeze-thaw cycles were considered inputs and the TCS was set as the system output. First, the ANN structure was optimized based on the GA. When there were 2 hidden layers, the first hidden layer and the second hidden layer had 14 and 11 neurons, respectively, and the RMSE was reduced to 1.562, which was much lower than the RMSE (3.522) based on the simple ANN model. Then, based on the optimal ANN structure (4-14-11-1), the initial connection weights and biases of the ANN were further optimized based on GA and the RMSE was minimized (1.083); thus, the optimal ANN model was obtained. After proposing the AI systems, to determine the accuracy level of the developed models, three performance indices including RMSE, MAE, and R^2 were used and computed. The RMSE, MAE, and R^2 equal to 1.083, 0.893, and 0.993, respectively, for testing datasets revealed the highest accuracy of the hybrid GA-ANN model in predicting TCS of sandstone subjected to freeze-thaw cycles, while these values were 2.676, 2.153, and 0.952 for the simple ANN model. These results indicated the superiority of the hybrid GA-ANN model in predicting TCS of sandstone subjected to freeze-thaw cycles in comparison with the simple ANN model.

Data Availability

The data are presented in the manuscript.

Conflicts of Interest

The authors declare that they have no conflict of interest.

Acknowledgments

This work was supported by the National Natural Science Foundation of China (Grant no. 51774323), the Hunan Provincial Natural Science Foundation of China (Grant no. 2020JJ4704), and the fundamental research funds for the central universities of Central South University, China (Grant no. 2021zzts0279).

References

[1] W. Chen, X. Tan, H. Yu, K. Yuan, and S. Li, "Advance and review on thermo-hydro-mechanical characteristics of rock mass under condition of low temperature and freeze-thaw cycles," *Chinese Journal of Rock Mechanics and Engineering*, vol. 30, no. 7, pp. 1318–1336, 2011.

[2] R.-H. Cao, C. Wang, R. Yao et al., "Effects of cyclic freeze-thaw treatments on the fracture characteristics of sandstone under different fracture modes: laboratory testing," *Theoretical and Applied Fracture Mechanics*, vol. 109, p. 102738, 2020.

[3] H. Zhang, C. Yuan, G. Yang et al., "A novel constitutive modelling approach measured under simulated freeze–thaw cycles for the rock failure," *Engineering with Computers*, vol. 37, pp. 779–792, 2019.

[4] F. Gao, X. Xiong, C. Xu, and K. Zhou, "Mechanical property deterioration characteristics and a new constitutive model for rocks subjected to freeze-thaw weathering process," *International Journal of Rock Mechanics and Mining Sciences*, vol. 140, p. 104642, 2021.

[5] X. Tan, W. Chen, J. Yang, and J. Cao, "Laboratory investigations on the mechanical properties degradation of granite under freeze-thaw cycles," *Cold Regions Science and Technology*, vol. 68, no. 3, pp. 130–138, 2011.

[6] M. Hosseini and A. R. Khodayari, "Effect of freeze-thaw cycle on strength and rock strength parameters (a Lushan sandstone case study)," *Journal of Mining and Environment*, vol. 10, no. 1, pp. 257–270, 2019.

[7] Y. Shen and X. Wang, "Study on freeze thawing and damage mechanism of rock in Western cold and dry area," *Urban Roads Bridges and Flood Control*, vol. 7, no. 9, pp. 223-224, 2017.

[8] Y. Bai, R. Shan, Y. Ju, Y. Wu, P. Sun, and Z. Wang, "Study on the mechanical properties and damage constitutive model of frozen weakly cemented red sandstone," *Cold Regions Science and Technology*, vol. 171, p. 102980, 2020.

[9] F. Bayram, "Predicting mechanical strength loss of natural stones after freeze-thaw in cold regions," *Cold Regions Science and Technology*, vol. 83-84, pp. 98–102, 2012.

[10] İ. İnce and M. Fener, "A prediction model for uniaxial compressive strength of deteriorated pyroclastic rocks due to freeze-thaw cycle," *Journal of African Earth Sciences*, vol. 120, pp. 134–140, 2016.

[11] Q. Liu, S. Huang, Y. Kang, and X. Liu, "A prediction model for uniaxial compressive strength of deteriorated rocks due to freeze-thaw," *Cold Regions Science and Technology*, vol. 120, pp. 96–107, 2015.

[12] H. Fu, J. Zhang, Z. Huang, Y. Shi, and W. Chen, "A statistical model for predicting the triaxial compressive strength of transversely isotropic rocks subjected to freeze-thaw cycling," *Cold Regions Science and Technology*, vol. 145, pp. 237–248, 2018.

[13] S. Z. Seyed Mousavi, H. Tavakoli, P. Moarefvand, and M. Rezaei, "Assessing the effect of freezing-thawing cycles on the results of the triaxial compressive strength test for calc-schist rock," *International Journal of Rock Mechanics and Mining Sciences*, vol. 123, p. 104090, 2020.

[14] D. J. Armaghani and E. Momeni, "Feasibility of ANFIS model for prediction of ground vibrations resulting from quarry blasting," *Environmental Earth Sciences*, vol. 74, no. 4, pp. 2845–2860, 2015.

[15] M. Monjezi, Z. Ahmadi, A. Y. Varjani, and M. Khandelwal, "Backbreak prediction in the Chadormalu iron mine using artificial neural network," *Neural Computing and Applications*, vol. 23, pp. 1101–1107, 2012.

[16] M. Khandelwal and T. N. Singh, "Predicting elastic properties of schistose rocks from unconfined strength using intelligent approach," *Arabian Journal of Geosciences*, vol. 4, pp. 435–442, 2011.

[17] E. T. Mohamad, D. J. Armaghani, E. Momeni, A. H. Yazdavar, and M. Ebrahimi, "Rock strength estimation: a PSO-based BP

approach," *Neural Computing and Applications*, vol. 30, pp. 1635–1646, 2018.

[18] D. Jahed Armaghani, M. F. Mohd Amin, S. Yagiz, R. S. Faradonbeh, and R. A. Abdullah, "Prediction of the uniaxial compressive strength of sandstone using various modeling techniques," *International Journal of Rock Mechanics and Mining Sciences*, vol. 85, pp. 174–186, 2016.

[19] A. Momeni, Y. Abdilor, G. R. Khanlari, M. Heidari, and A. A. Sepahi, "The effect of freeze–thaw cycles on physical and mechanical properties of granitoid hard rocks," *Bulletin of Engineering Geology and the Environment*, vol. 75, pp. 1649–1656, 2015.

[20] X.-C. Qin, S.-P. Meng, D.-F. Cao et al., "Evaluation of freeze-thaw damage on concrete material and prestressed concrete specimens," *Construction and Building Materials*, vol. 125, pp. 892–904, 2016.

[21] Z. Pan, K. Zhou, R. Gao et al., "Research on the pore evolution of sandstone in cold regions under freeze-thaw weathering cycles based on NMR," *Geofluids*, vol. 2020, Article ID 8849444, 12 pages, 2020.

[22] J.-L. Li, K.-P. Zhou, W.-J. Liu, and H.-W. Deng, "NMR research on deterioration characteristics of microscopic structure of sandstones in freeze-thaw cycles," *Transactions of Nonferrous Metals Society of China*, vol. 26, no. 11, pp. 2997–3003, 2016.

[23] N. Efkolidis, A. Markopoulos, N. Karkalos, C. G. Hernández, J. L. H. Talón, and P. Kyratsis, "Optimizing models for sustainable drilling operations using genetic algorithm for the optimum ANN," *Applied Artificial Intelligence*, vol. 33, no. 10, pp. 881–901, 2019.

[24] M. Khandelwal, A. Marto, S. A. Fatemi et al., "Implementing an ANN model optimized by genetic algorithm for estimating cohesion of limestone samples," *Engineering with Computers*, vol. 34, pp. 307–317, 2018.

[25] Z. Shao, D. Jahed Armaghani, B. Yazdani Bejarbaneh, M. A. Mu'azu, and E. Tonnizam Mohamad, "Estimating the friction angle of black shale core specimens with hybrid-ANN approaches," *Measurement*, vol. 145, pp. 744–755, 2019.

[26] C. Qi, A. Fourie, and Q. Chen, "Neural network and particle swarm optimization for predicting the unconfined compressive strength of cemented paste backfill," *Construction and Building Materials*, vol. 159, pp. 473–478, 2018.

[27] J. H. Holland, "Genetic algorithms and the optimal allocation of trials," *SIAM Journal on Computing*, vol. 2, no. 2, pp. 88–105, 1973.

[28] D. E. Goldberg, *Genetic Algorithm in Search, Optimization, and Machine Learning*, The University of Alabama, Addison-Wesley Publishing Company, 1989.

[29] J. Arifovic and R. Gencay, "Using genetic algorithms to select architecture of a feedforward artificial neural network," *Physica A: Statistical Mechanics and its Applications*, vol. 289, no. 3-4, pp. 574–594, 2001.

[30] Q. H. Doan, T. Le, and D.-K. Thai, "Optimization strategies of neural networks for impact damage classification of RC panels in a small dataset," *Applied Soft Computing*, vol. 102, p. 107100, 2021.

[31] A. C. Bahnsen and A. M. Gonzalez, "Evolutionary algorithms for selecting the architecture of a MLP neural network: a credit scoring case," in *2011 IEEE 11th International Conference on Data Mining Workshops*, pp. 725–732, 2011.

[32] F. Boithias, M. El Mankibi, and P. Michel, "Genetic algorithms based optimization of artificial neural network architecture for buildings' indoor discomfort and energy consumption prediction," *Building Simulation*, vol. 5, no. 2, pp. 95–106, 2012.

[33] J. Idrissi, R. Hassan, C. Youssef, and E. Mohamed, *Genetic Algorithm for Neural Network Architecture Optimization*, Third International Conference on Logistics Operations Management, IEEE, 2016.

[34] C. Jeong, J. H. Min, and M. S. Kim, "A tuning method for the architecture of neural network models incorporating GAM and GA as applied to bankruptcy prediction," *Expert Systems with Applications*, vol. 39, no. 3, pp. 3650–3658, 2012.

[35] M. Khandelwal, "Blast-induced ground vibration prediction using support vector machine," *Engineering with Computers*, vol. 27, pp. 193–200, 2011.

[36] X. Lu, W. Zhou, X. Ding, X. Shi, B. Luan, and M. Li, "Ensemble learning regression for estimating unconfined compressive strength of cemented paste backfill," *IEEE Access*, vol. 7, pp. 72125–72133, 2019.

[37] R. Hecht-Nielsen, *Kolmogorov's Mapping Neural Network Existence Theorem*, The first IEEE international conference on neural networks, IEEE, 1987.

[38] K. Hornik, M. Stinchcombe, and H. White, "Multilayer feedforward networks are universal approximators," *Neural Networks*, vol. 2, no. 5, pp. 359–366, 1989.

[39] Z. H. Zhang, D. N. Yan, J. T. Ju, and Y. Han, "Prediction of the flow stress of a high alloyed austenitic stainless steel using artificial neural network," *Materials Science Forum*, vol. 724, pp. 351–354, 2012.

[40] B. D. Ripley, *Statistical Aspects of Neural Networks*, Springer, USA, 1993.

[41] J. Paola, *Neural network classification of multispectral imagery, [M.S. thesis]*, The University of Arizona, USA, 1994.

[42] C. Wang, *A theory of generalization in learning machines with neural application, [Ph.D. thesis]*, The University of Pennsylvania, USA, 1994.

[43] T. Masters, *Practical Neural Network Recipes in C++*, Academic Press, USA, 1993.

[44] I. Kaastra and M. Boyd, "Designing a neural network for forecasting financial and economic time series," *Neurocomputing*, vol. 10, pp. 215–236, 1996.

[45] I. Kanellopoulos and G. G. Wilkinson, "Strategies and best practice for neural network image classification," *International Journal of Remote Sensing*, vol. 18, no. 4, pp. 711–725, 2010.

[46] C. Qi, Q. Chen, A. Fourie, and Q. Zhang, "An intelligent modelling framework for mechanical properties of cemented paste backfill," *Minerals Engineering*, vol. 123, pp. 16–27, 2018.

[47] K. Zorlu, C. Gokceoglu, F. Ocakoglu, H. A. Nefeslioglu, and S. Acikalin, "Prediction of uniaxial compressive strength of sandstones using petrography- based models," *Engineering Geology*, vol. 96, no. 3-4, pp. 141–158, 2008.